Computing 64, 323–338 (2000)

Computing

Gauss–Newton Multilevel Methods for Least-Squares Finite Element Computations of Variably Saturated Subsurface Flow

G. Starke, Essen

Received January 4, 1999; revised July 19, 1999

Abstract

We apply the least-squares mixed finite element framework to the nonlinear elliptic problems arising in each time-step of an implicit Euler discretization for variably saturated flow. This approach allows the combination of standard piecewise linear H^1-conforming finite elements for the hydraulic potential with the $H(\mathrm{div})$-conforming Raviart–Thomas spaces for the flux. It also provides an a posteriori error estimator which may be used in an adaptive mesh refinement strategy. The resulting nonlinear algebraic least-squares problems are solved by an inexact Gauss–Newton method using a stopping criterion for the inner iteration which is based on the change of the linearized least-squares functional relative to the nonlinear least-squares functional. The inner iteration is carried out using an adaptive multilevel method with a block Gauss–Seidel smoothing iteration. For a realistic water table recharge problem, the results of computational experiments are presented.

AMS Subject Classifications: 65M55, 65M60, 76S05.

Key Words: Variably saturated flow, nonlinear elliptic problems, least-squares finite element method, inexact Gauss–Newton method, Raviart–Thomas spaces, multilevel method.

1. Introduction

Variably saturated subsurface flow problems arise, for example, in the modelling of infiltration problems in soil mechanics. A widely used model is based on two first-order differential equations which stand for mass conservation (scalar equation) and a generalization of Darcy's law (vector equation) for the two process variables, namely, the hydraulic potential (scalar unknown) and volumetric flux (vector unknown). This model is often used in combination with a parametrization proposed by Mualem [11] and Van Genuchten [15]. Mathematically, this is equivalent to a nonlinear parabolic initial-boundary value problem, which is possibly degenerate, for the scalar variable (hydraulic potential). Since one is also interested in accurate approximations to the vector variable (flux), it is appropriate to work directly with the first-order system as a starting point for the numerical method. After an implicit discretization of the time derivative, we obtain the first-order system formulation of a nonlinear elliptic boundary value problem. For this problem, we use a least-squares mixed finite element approach which simultaneously constructs approximations to the scalar and vector variables in appropriate finite element spaces.

A detailed study of the least-squares finite element method applied to the nonlinear variably saturated subsurface flow problem described above is given in [14]. One of its important properties is that the local evaluation of the nonlinear least-squares functional serves as an a posteriori error estimator to be used in an adaptive refinement process. In [14], the (exact) Gauss–Newton method was used to solve the algebraic least-squares problems arising from the least-squares finite element approach. Here, we use an inexact Gauss–Newton method where the linear least-squares problems arising in each step are solved using an adaptive multilevel V-cycle algorithm. Nonlinear multilevel methods for this type of least-squares computations are studied in [10]. Our purpose in this paper is twofold: Firstly, we provide a stopping criterion for the inner iteration and, secondly, we study and compare two smoothing iterations to be used in the adaptive multilevel V-cycle algorithm. Our stopping criterion is based on the change of the linearized least-squares functional relative to the nonlinear least-squares functional which gives the proper balance between algebraic and discretization error. Such a stopping criterion is crucial for an efficient overall solution strategy since this part constitutes the main computational work. The smoothing iterations are two adaptive variants of those introduced by Arnold, Falk and Winther [1] adapted to the least-squares framework.

A comparison of the least-squares method used here to the Raviart–Thomas mixed method [12] and to standard Galerkin methods for the equivalent second-order elliptic problem is beyond the scope of this paper. Note that such a comparison depends on the process variables of interest and on the choice of norm in which accuracy is measured. If it is desirable to approximate the flux in $H(\mathrm{div}, \Omega)$, then the use of mixed methods is mandatory.

The following section presents the background on the least-squares formulation for the nonlinear first-order systems arising in each time-step of the variably saturated subsurface flow problem. In Section 3, some practical considerations for the inexact Gauss–Newton method are studied. In particular, we derive a stopping criterion for the inner iteration based on the change of the linearized least-squares functional relative to the nonlinear least-squares functional. Section 4 is concerned with adaptive multilevel methods for the solution of the linear least-squares problems arising in each Gauss–Newton step. Here, two types of smoothing iterations are defined from the least-squares principles. Finally, computational experiments for a realistic water table recharge problem are presented in Section 5 which illustrate the effectiveness of the adaptive Gauss–Newton multilevel method.

2. Nonlinear Least-Squares Finite Element Formulation

Variably saturated subsurface flow may be modelled by the first-order system

$$\begin{aligned} \partial_t \theta(p) + \mathrm{div}\, u &= 0 \\ u + K(p)\nabla p &= 0 \end{aligned} \tag{1}$$

for the hydraulic potential $p : [0,T] \times \Omega \to \mathbb{R}$ and the volumetric flux $u : [0,T] \times \Omega \to \mathbb{R}^2$ in a domain $\Omega \subset \mathbb{R}^2$ subject to initial and boundary conditions. The water content $\theta(p)$ and the permeability $K(p)$ are nonlinear functions of p given by the model of Mualem [11] and Van Genuchten [15]. The first equation in (1) stands for conservation of mass, the second one which links flux to pressure is the Buckingham–Darcy law (see, for example, [9, Sect. 3.3]). At time $t = 0$, we have an initial condition for the hydraulic potential. The boundary of Ω is divided into two parts $\partial\Omega = \Gamma_N \cup \Gamma_D$ where, for all $t \in (0,T]$, the hydraulic potential p and the normal flux $n \cdot u$ is prescribed on Γ_D and Γ_N, respectively.

Discretizing in time by an implicit Euler scheme leads to the system

$$\frac{\theta(p) - \theta(p^{\text{old}})}{\tau} + \operatorname{div} u = 0$$

$$u + K(p)\nabla p = 0$$

for u and p with $n \cdot u = n \cdot u^N$ on Γ_N and $p = p^D$ on Γ_D at the new time-step $t = t^{\text{old}} + \tau$. We may rescale these two equations and end up with

$$\mathscr{R}(p,u) = \begin{pmatrix} \theta(p) - \theta(p^{\text{old}}) + \tau \operatorname{div} u \\ \sqrt{\tau}(u + K(p)\nabla p) \end{pmatrix} = 0. \tag{2}$$

The particular scaling in the first-order system (2) is motivated by the aim for ellipticity estimates which are uniform in τ. This will be explored further in [13]. Let $p^D \in H^1(\Omega)$ and $u^N \in H(\operatorname{div},\Omega)$ be such that the boundary conditions on Γ_D for p^D and on Γ_N for $n \cdot u_N$ are fulfilled. If we define the spaces

$$Q := \{q \in H^1(\Omega) : q = 0 \text{ on } \Gamma_D\},$$

$$V := \{v \in H(\operatorname{div},\Omega) : n \cdot v = 0 \text{ on } \Gamma_N\},$$

then we are interested in solutions of (2) of the form $p = p^D + \hat{p}$, $u = u^N + \hat{u}$ with $\hat{p} \in Q, \hat{u} \in V$. Note that the nonlinear coefficient functions $\theta(p)$ and $K(p)$ are such that $\mathscr{R} : Q \times V \to (L^2(\Omega))^3$. Under the assumption that the equation $\mathscr{R}(p^D + \hat{p}, u^N + \hat{u}) = 0$ has a unique solution $(\hat{p}, \hat{u}) \in Q \times V$, this solution is the unique minimizer of the least-squares functional

$$\|\mathscr{R}(p^D + \hat{p}, u^N + \hat{u})\|^2_{0,\Omega}$$

and the minimum value is zero. The least-squares finite element approach attempts to minimize this least-squares functional approximately in finite-dimensional spaces $Q_h \subset Q, V_h \subset V$. We compute approximate solutions $p_h = p^D + \hat{p}_h$ and $u_h = u^N + \hat{u}_h$ with $\hat{p}_h \in Q_h$ and $\hat{u}_h \in V_h$ such that

$$\|\mathscr{R}(p^D + \hat{p}_h, u^N + \hat{u}_h)\|^2_{0,\Omega} = \min_{\hat{q}_h \in Q_h, \hat{v}_h \in V_h} \|\mathscr{R}(p^D + \hat{q}_h, u^N + \hat{v}_h)\|^2_{0,\Omega} \tag{3}$$

holds. Since $\mathscr{R}(p^D + \hat{p}, u^N + \hat{u}) = 0$ for the exact solution $(\hat{p}, \hat{u}) \in Q \times V$, we have

$$
\begin{aligned}
&\|\mathscr{R}(p^D+\hat{p}_h,u^N+\hat{u}_h)\|_{0,\Omega}^2\\
&\quad=\|\mathscr{R}(p^D+\hat{p}_h,u^N+\hat{u}_h)-\mathscr{R}(p^D+\hat{p},u^N+\hat{u})\|_{0,\Omega}^2\\
&\quad=\left\|\begin{pmatrix}\theta(p^D+\hat{p}_h)-\theta(p^D+\hat{p})+\tau\mathrm{div}(\hat{u}_h-\hat{u})\\ \sqrt{\tau}(\hat{u}_h-\hat{u}+K(p^D+\hat{p}_h)\nabla(p^D+\hat{p}_h)-K(p^D+\hat{p})\nabla(p^D+\hat{p}))\end{pmatrix}\right\|_{0,\Omega}^2\\
&\quad\approx\left\|\begin{pmatrix}\theta'(p^D+\hat{p})(\hat{p}_h-\hat{p})+\tau\mathrm{div}(\hat{u}_h-\hat{u})\\ \sqrt{\tau}(\hat{u}_h-\hat{u}+\nabla(K(p^D+\hat{p})(\hat{p}_h-\hat{p})))\end{pmatrix}\right\|_{0,\Omega}^2.
\end{aligned}
$$

This linearized problem falls into the framework studied in [5] where coercivity and continuity with respect to the $H^1(\Omega)\times H(\mathrm{div},\Omega)$ norm is proved. This means that if (p_h,u_h) is sufficiently close to (p,u), then the minimum of the least-squares functional in (3) is itself an error measure. The dependence of the coercivity and continuity constants on τ with respect to particular scaled norms is studied in [13].

If we accept the least-squares functional as an appropriate error measure, then it also constitutes an a posteriori error estimator. This is due to the simple fact that the functional is the sum of its local contributions, i.e.,

$$
\|\mathscr{R}(p^D+\hat{p}_h,u^N+\hat{u}_h)\|_{0,\Omega}^2=\sum_{T\in\mathscr{T}_h}\|\mathscr{R}(p^D+\hat{p}_h,u^N+\hat{u}_h)\|_{0,T}^2.
$$

Since this approach is based on the local evaluation of the nonlinear least-squares functional, the error for the nonlinear problem is estimated directly and no linearization is necessary. Another advantage is that the local contributions of the least-squares functional are a part of the computations of the solution method so that there is no additional work necessary for evaluating the error estimator.

For some prescribed tolerance ε for the discretization error, our goal is to achieve

$$
\|\mathscr{R}(p^D+\hat{p}_h,u^N+\hat{u}_h)\|_{0,\Omega}^2\le\varepsilon
$$

with the least computational effort, i.e., the smallest number of points in the triangulation. To this end, we refine those triangles with

$$
\|\mathscr{R}(p^D+\hat{p}_h,u^N+\hat{u}_h)\|_{0,T}^2>\frac{\varepsilon}{\#T},
$$

where $\#T$ is the number of triangles in the current triangulation. Other refinement strategies based on the least-squares approach are discussed in [2].

3. Inexact Gauss–Newton Method

The Gauss–Newton method computes successive approximations to the nonlinear least-squares problem by solving a sequence of linear least-squares problems. In the k-th step, the current iterate $(p_h^{(k)},u_h^{(k)})$ is replaced by an update

$(p_h^{(k+1)}, u_h^{(k+1)}) = (p_h^{(k)} + \delta p_h, u_h^{(k)} + \delta u_h)$ with $\delta p_h \in Q_h, \delta u_h \in V_h$ such that the least-squares functional is reduced. Linear approximation leads to

$$\begin{aligned}\mathscr{R}(p_h^{(k)} + \delta p_h, u_h^{(k)} + \delta u_h) &\approx \begin{pmatrix} \theta(p_h^{(k)}) - \theta(p^{\text{old}}) + \tau \operatorname{div} u_h^{(k)} \\ \sqrt{\tau}(u_h^{(k)} + K(p_h^{(k)})\nabla p_h^{(k)}) \end{pmatrix} \\ &\quad + \begin{pmatrix} \theta'(p_h^{(k)})\delta p_h + \tau \operatorname{div} \delta u_h \\ \sqrt{\tau}(\delta u_h + K'(p_h^{(k)})\nabla p_h^{(k)} \delta p_h + K(p_h^{(k)})\nabla \delta p_h) \end{pmatrix} \\ &=: \mathscr{R}(p_h^{(k)}, u_h^{(k)}) + \mathscr{J}(p_h^{(k)}, u_h^{(k)}) \begin{pmatrix} \delta p_h \\ \delta u_h \end{pmatrix}. \end{aligned} \tag{4}$$

Note that, for fixed $(p_h^{(k)}, u_h^{(k)}) \in H^1(\Omega) \times H(\operatorname{div}, \Omega)$, the mapping

$$\mathscr{J}(p_h^{(k)}, u_h^{(k)}) : Q_h \times V_h \to (L^2(\Omega))^3$$

is linear. Minimizing the linearized least-squares functional

$$\left\| \mathscr{R}(p_h^{(k)}, u_h^{(k)}) + \mathscr{J}(p_h^{(k)}, u_h^{(k)}) \begin{pmatrix} \delta p_h \\ \delta u_h \end{pmatrix} \right\|_{0,\Omega}^2$$

is equivalent to finding $\delta p_h \in Q_h$ and $\delta u_h \in V_h$ such that

$$\left(\mathscr{R}(p_h^{(k)}, u_h^{(k)}) + \mathscr{J}(p_h^{(k)}, u_h^{(k)}) \begin{pmatrix} \delta p_h \\ \delta u_h \end{pmatrix}, \mathscr{J}(p_h^{(k)}, u_h^{(k)}) \begin{pmatrix} \hat{q}_h \\ \hat{v}_h \end{pmatrix} \right)_{0,\Omega} = 0 \tag{5}$$

for all $(\hat{q}_h, \hat{v}_h) \in Q_h \times V_h$.

The nonlinear least-squares problem (3) is equivalent to the variational problem

$$\left(\mathscr{R}(p^D + \hat{p}_h, u^N + \hat{u}_h), \mathscr{J}(p^D + \hat{p}_h, u^N + \hat{u}_h) \begin{pmatrix} \hat{q}_h \\ \hat{v}_h \end{pmatrix} \right)_{0,\Omega} = 0 \tag{6}$$

for all $(\hat{q}_h, \hat{v}_h) \in Q_h \times V_h$. With respect to the nodal bases $\{\phi_h^{(\nu)}\}_{\nu=1}^{M_h}$ for Q_h and $\{\psi_h^{(\nu)}\}_{\nu=1}^{N_h}$ for V_h, this leads to the definition of the residual

$$\begin{aligned} r(p_h^{(k)}, u_h^{(k)}) = \Bigg(&\sum_{\nu=1}^{M_h} \left(\mathscr{R}(p_h^{(k)}, u_h^{(k)}), \mathscr{J}(p_h^{(k)}, u_h^{(k)}) \begin{pmatrix} \phi_h^{(\nu)} \\ 0 \end{pmatrix} \right)_{0,\Omega}^2 \\ &+ \sum_{\nu=1}^{N_h} \left(\mathscr{R}(p_h^{(k)}, u_h^{(k)}), \mathscr{J}(p_h^{(k)}, u_h^{(k)}) \begin{pmatrix} 0 \\ \psi_h^{(\nu)} \end{pmatrix} \right)_{0,\Omega}^2 \Bigg)^{1/2}. \end{aligned} \tag{7}$$

The Gauss–Newton iteration is stopped as soon as the nonlinear residual in (7) satisfies

$$r(p_h^{(k)}, u_h^{(k)}) \leq \eta h \|\mathscr{R}(p_h^{(k)}, u_h^{(k)})\|_{0,\Omega},$$

where $0 < \eta \leq 1$ is some specified parameter, for example, $\eta = 0.1$. With this, the nonlinear algebraic residual is linked to the nonlinear least-squares functional which measures the total error with respect to the solution of the variational problem. The factor h (representing the mesh-size) is thought to fill the gap between the norm in (7) and the norm of the residual in the dual space of $H^1(\Omega) \times H(\mathrm{div}, \Omega)$. We also use the nonlinear residual in a damping strategy in order to get global convergence of the Gauss–Newton method in the following way (cf. [7, Algorithm 6.3.5]): Successively choose μ_k from $\{1, 1/2, 1/4, \ldots, \mu_{\min}\}$ and set

$$(p_h^{(k+1)}, u_h^{(k+1)}) = (p_h^{(k)} + \mu_k \delta p_h, u_h^{(k)} + \mu_k \delta u_h)$$

until

$$\begin{aligned} &\|\mathscr{R}(p_h^{(k)} + \mu_k \delta p_h, u_h^{(k)} + \mu_k \delta u_h)\|_{0,\Omega}^2 \\ &\quad \leq \|\mathscr{R}(p_h^{(k)}, u_h^{(k)})\|_{0,\Omega}^2 - \alpha \mu_k (r(p_h^{(k)}, u_h^{(k)}))^2 \end{aligned}$$

(with $\alpha = 10^{-4}$) is fulfilled.

The linear least-squares problems arising in each Gauss–Newton step may be solved using the multilevel methods described in the next section. Let us denote the inner iterations for solving the linear least-squares problem in the k-th Gauss–Newton step by

$$(p_h^{(k)} + \delta p_h^{(\kappa)}, u_h^{(k)} + \delta u_h^{(\kappa)}) =: (p_h^{(k,\kappa)}, u_h^{(k,\kappa)}), \quad \kappa = 0, 1, \ldots$$

with $(\delta p_h^{(0)}, \delta u_h^{(0)}) = (0, 0)$. The stopping criterion for this inner iteration is based on the change in the linear least-squares functional relative to the size of the nonlinear least-squares functional. In particular, the iteration may be stopped as soon as the condition

$$\begin{aligned} &\left\| \mathscr{R}(p_h^{(k)}, u_h^{(k)}) + \mathscr{J}(p_h^{(k)}, u_h^{(k)}) \begin{pmatrix} \delta p_h^{(\kappa-1)} \\ \delta u_h^{(\kappa-1)} \end{pmatrix} \right\|_{0,\Omega} \\ &\quad - \left\| \mathscr{R}(p_h^{(k)}, u_h^{(k)}) + \mathscr{J}(p_h^{(k)}, u_h^{(k)}) \begin{pmatrix} \delta p_h^{(\kappa)} \\ \delta u_h^{(\kappa)} \end{pmatrix} \right\|_{0,\Omega} \leq \eta \|\mathscr{R}(p_h^{(k,\kappa)}, u_h^{(k,\kappa)})\|_{0,\Omega} \end{aligned} \tag{8}$$

is fulfilled. In other words, the inner iteration is stopped when the algebraic residual reduction does not lead to a significant reduction of the linearized least-squares functional anymore.

Theorem 1. *Let $(\delta p_h, \delta u_h) \in Q_h \times V_h$ be the exact solution of the linearized least-squares problem, and assume that*

$$\left\| \mathcal{J}(p_h^{(k)}, u_h^{(k)}) \begin{pmatrix} \delta p_h^{(\kappa)} - \delta p_h \\ \delta u_h^{(\kappa)} - \delta u_h \end{pmatrix} \right\|_{0,\Omega} \leq \rho \left\| \mathcal{J}(p_h^{(k)}, u_h^{(k)}) \begin{pmatrix} \delta p_h^{(\kappa-1)} - \delta p_h \\ \delta u_h^{(\kappa-1)} - \delta u_h \end{pmatrix} \right\|_{0,\Omega} \tag{9}$$

holds for $\kappa = 1, 2, \ldots$. In other words, the inner iteration satisfies a uniform error reduction by a factor of ρ. If (8) *is fulfilled, then*

$$\begin{aligned} &\left\| \mathcal{J}(p_h^{(k)}, u_h^{(k)}) \begin{pmatrix} \delta p_h^{(\kappa)} - \delta p_h \\ \delta u_h^{(\kappa)} - \delta u_h \end{pmatrix} \right\|_{0,\Omega}^2 \\ &\quad \leq \frac{\eta \rho^{\kappa+1}}{1-\rho} \|\mathcal{R}(p_h^{(k)}, u_h^{(k)})\|_{0,\Omega} \|\mathcal{R}(p_h^{(k,\kappa)}, u_h^{(k,\kappa)})\|_{0,\Omega} \end{aligned} \tag{10}$$

Proof: By $(\delta p, \delta u) \in Q \times V$ we denote the solution of

$$\mathcal{R}(p_h^{(k)}, u_h^{(k)}) + \mathcal{J}(p_h^{(k)}, u_h^{(k)}) \begin{pmatrix} \delta p \\ \delta u \end{pmatrix} = \begin{pmatrix} 0 \\ 0 \end{pmatrix}.$$

Note that there exists a unique solution to this problem since from (4) it is first-order system formulation of a linear second-order elliptic problem. The Galerkin condition (5) implies

$$\left(\mathcal{J}(p_h^{(k)}, u_h^{(k)}) \begin{pmatrix} \delta p - \delta p_h \\ \delta u - \delta u_h \end{pmatrix}, \mathcal{J}(p_h^{(k)}, u_h^{(k)}) \begin{pmatrix} q_h \\ v_h \end{pmatrix} \right)_{0,\Omega} = 0$$

for all $(a_h, v_h) \in Q_h \times V_h$. Combined with (9) and

$$\left\| \mathcal{R}(p_h^{(k)}, u_h^{(k)}) + \mathcal{J}(p_h^{(k)}, u_h^{(k)}) \begin{pmatrix} \delta p_h^{(\kappa)} \\ \delta u_h^{(\kappa)} \end{pmatrix} \right\|_{0,\Omega} \leq \rho^{\kappa} \|\mathcal{R}(p_h^{(k)}, u_h^{(k)})\|_{0,\Omega}$$

for $\kappa = 1, 2, \ldots$, this leads to

$$\begin{aligned} &\rho^{\kappa} \left(\frac{1}{\rho} + 1 \right) \|\mathcal{R}(p_h^{(k)}, u_h^{(k)})\|_{0,\Omega} \\ &\quad \times \left(\left\| \mathcal{R}(p_h^{(k)}, u_h^{(k)}) + \mathcal{J}(p_h^{(k)}, u_h^{(k)}) \begin{pmatrix} \delta p_h^{(\kappa-1)} \\ \delta u_h^{(\kappa-1)} \end{pmatrix} \right\|_{0,\Omega} \right. \\ &\quad \left. - \left\| \mathcal{R}(p_h^{(k)}, u_h^{(k)}) + \mathcal{J}(p_h^{(k)}, u_h^{(k)}) \begin{pmatrix} \delta p_h^{(\kappa)} \\ \delta u_h^{(\kappa)} \end{pmatrix} \right\|_{0,\Omega} \right) \end{aligned}$$

$$
\begin{aligned}
&\geq \left\| \mathscr{R}(p_h^{(k)}, u_h^{(k)}) + \mathscr{J}(p_h^{(k)}, u_h^{(k)}) \begin{pmatrix} \delta p_h^{(\kappa-1)} \\ \delta u_h^{(\kappa-1)} \end{pmatrix} \right\|_{0,\Omega}^2 \\
&\quad - \left\| \mathscr{R}(p_h^{(k)}, u_h^{(k)}) + \mathscr{J}(p_h^{(k)}, u_h^{(k)}) \begin{pmatrix} \delta p_h^{(\kappa)} \\ \delta u_h^{(\kappa)} \end{pmatrix} \right\|_{0,\Omega}^2 \\
&= \left\| \mathscr{J}(p_h^{(k)}, u_h^{(k)}) \begin{pmatrix} \delta p_h^{(\kappa-1)} - \delta p \\ \delta u_h^{(\kappa-1)} - \delta u \end{pmatrix} \right\|_{0,\Omega}^2 + \left\| \mathscr{J}(p_h^{(k)}, u_h^{(k)}) \begin{pmatrix} \delta p_h^{(\kappa)} - \delta p \\ \delta u_h^{(\kappa)} - \delta u \end{pmatrix} \right\|_{0,\Omega}^2 \\
&= \left\| \mathscr{J}(p_h^{(k)}, u_h^{(k)}) \begin{pmatrix} \delta p_h^{(\kappa-1)} - \delta p_h \\ \delta u_h^{(\kappa-1)} - \delta u_h \end{pmatrix} \right\|_{0,\Omega}^2 + \left\| \mathscr{J}(p_h^{(k)}, u_h^{(k)}) \begin{pmatrix} \delta p_h - \delta p \\ \delta u_h - \delta u \end{pmatrix} \right\|_{0,\Omega}^2 \\
&\quad - \left\| \mathscr{J}(p_h^{(k)}, u_h^{(k)}) \begin{pmatrix} \delta p_h^{(\kappa)} - \delta p_h \\ \delta u_h^{(\kappa)} - \delta u_h \end{pmatrix} \right\|_{0,\Omega}^2 + \left\| \mathscr{J}(p_h^{(k)}, u_h^{(k)}) \begin{pmatrix} \delta p_h - \delta p \\ \delta u_h - \delta u \end{pmatrix} \right\|_{0,\Omega}^2 \\
&= \left\| \mathscr{J}(p_h^{(k)}, u_h^{(k)}) \begin{pmatrix} \delta p_h^{(\kappa-1)} - \delta p_h \\ \delta u_h^{(\kappa-1)} - \delta u_h \end{pmatrix} \right\|_{0,\Omega}^2 + \left\| \mathscr{J}(p_h^{(k)}, u_h^{(k)}) \begin{pmatrix} \delta p_h^{(\kappa)} - \delta p_h \\ \delta u_h^{(\kappa)} - \delta u_h \end{pmatrix} \right\|_{0,\Omega}^2 \\
&\geq \left(\frac{1}{\rho^2} - 1 \right) \left\| \mathscr{J}(p_h^{(k)}, u_h^{(k)}) \begin{pmatrix} \delta p_h^{(\kappa)} - \delta p_h \\ \delta u_h^{(\kappa)} - \delta u_h \end{pmatrix} \right\|_{0,\Omega}^2 . \quad \square
\end{aligned}
$$

In particular, Theorem 1 states that if an iterative method is used for the linear least-squares problems which converges uniformly with respect to h, then the stopping criterion (8) is useful with η independent of h. We will see that the adaptive multilevel methods presented in the following section have this property.

4. Multilevel Solution of the Linear Least-Squares Problems

The adaptive refinement technique described in Section 2 constructs a sequence of triangulations $\mathscr{T}_{h_0}, \ldots, \mathscr{T}_{h_L}$. By $Q_{h_0}, \ldots, Q_{h_L}$ and $V_{h_0}, \ldots, V_{h_L}$ we denote the corresponding subspaces of Q and V, respectively. We utilize this sequence of triangulations in an adaptive multilevel V-cycle algorithm (see e.g. Braess [3, Chap. V]) for the solution of the linear least-squares problems. In the finite element framework, the transfer between levels is given canonically by the sequence of spaces (see, e.g. [3, Chap. V]). We restrict ourselves to standard continuous piecewise linear finite elements for Q_{h_l} and Raviart–Thomas spaces of lowest order (cf. [4, Section III.3.3]) for V_{h_l}. In order to compute a coarse space correction $(\tilde{\delta}p_{h_{l-1}}, \tilde{\delta}u_{h_{l-1}}) \in Q_{h_{l-1}} \times V_{h_{l-1}}$ to $(\tilde{\delta}p_{h_l}, \tilde{\delta}u_{h_l}) \in Q_{h_l} \times V_{h_l}$, we need to consider the least-squares problem

$$
\min_{\tilde{\delta}p_{h_{l-1}}, \tilde{\delta}u_{h_{l-1}}} \left\| \mathscr{R}(p_{h_l}^{(k)}, u_{h_l}^{(k)}) + \mathscr{J}(p_{h_l}^{(k)}, u_{h_l}^{(k)}) \begin{pmatrix} \tilde{\delta}p_{h_l} + \tilde{\delta}p_{h_{l-1}} \\ \tilde{\delta}u_{h_l} + \tilde{\delta}u_{h_{l-1}} \end{pmatrix} \right\|_{0,\Omega}^2 .
$$

The corresponding variational formulation for $\tilde{\delta p}_{h_{l-1}}, \tilde{\delta u}_{h_{l-1}}$ is

$$\left(\mathcal{J}(p_h^{(k)}, u_h^{(k)}) \begin{pmatrix} \tilde{\delta p}_{h_{l-1}} \\ \tilde{\delta u}_{h_{l-1}} \end{pmatrix}, \mathcal{J}(p_h^{(k)}, u_h^{(k)}) \begin{pmatrix} \hat{q}_{h_{l-1}} \\ \hat{v}_{h_{l-1}} \end{pmatrix} \right)_{0,\Omega}$$
$$= -\left(\mathcal{J}(p_h^{(k)}, u_h^{(k)}) \begin{pmatrix} \tilde{\delta p}_{h_l} \\ \tilde{\delta u}_{h_l} \end{pmatrix} + \mathcal{R}(p_h^{(k)}, u_h^{(k)}), \mathcal{J}(p_h^{(k)}, u_h^{(k)}) \begin{pmatrix} \hat{q}_{h_{l-1}} \\ \hat{v}_{h_{l-1}} \end{pmatrix} \right)_{0,\Omega} \tag{11}$$

for all $(\hat{q}_{h_{l-1}}, \hat{v}_{h_{l-1}}) \in Q_{h_{l-1}} \times V_{h_{l-1}}$. This is implemented using the interpolation and restriction operators with respect to the sequence of finite element spaces.

In order to define the smoothing iteration, we consider the variational problem on the fine level l in matrix form

$$\begin{pmatrix} \mathbf{A}_{pp} & \mathbf{A}_{pu} \\ \mathbf{A}_{pu}^T & \mathbf{A}_{uu} \end{pmatrix} \begin{pmatrix} \mathbf{p} \\ \mathbf{u} \end{pmatrix} = \begin{pmatrix} \mathbf{f}_p \\ \mathbf{f}_u \end{pmatrix}.$$

The block $\mathbf{A}_{pp} \in \mathbb{R}^{M_{h_l} \times M_{h_l}}$ denotes the discretization of an $H^1(\Omega)$-elliptic problem while $\mathbf{A}_{uu} \in \mathbb{R}^{N_{h_l} \times N_{h_l}}$ stands for an operator defined in $H(\mathrm{div}, \Omega)$. Standard point Gauss–Seidel smoothing is therefore expected to be effective for the pressure unknowns in $\mathbf{p}$. For the unknowns associated with the flux $\mathbf{u}$ we need to eliminate those divergence-free error components which are not visible on the coarser triangulations. This is done using the Gauss–Seidel version of the method by Arnold, Falk and Winther which consists in solving, consecutively for all points, the small subproblems associated with the normal flux on all edges adjacent to this point. This defines the first Gauss–Seidel type smoothing method to be used in our multilevel algorithm. We may formulate this smoothing iteration as successive subspace correction in the following way: For all points $x_l^{(v)}, v = 1, \ldots, M'_{h_l}$ of the triangulation $\mathcal{T}_{h_l}$ (note that $M'_{h_l} > M_{h_l}$, in general), we define the local subregion $\Omega_l^{(v)}$ as the union of all triangles which have $x_l^{(v)}$ as vertex. Next, we define the local subspaces

$$Q_l^{(v)} := \{q \in Q_{h_l} : \mathrm{supp}\ q \subseteq \Omega_l^{(v)}\}$$
$$V_l^{(v)} := \{v \in V_{h_l} : \mathrm{supp}\ v \subseteq \Omega_l^{(v)}\}.$$

The left graph in Fig. 1 shows one such local subdomain $\Omega_l^{(v)}$ (as shaded region). The associated space $Q_l^{(v)}$ is spanned by the basis function $\phi_{h_l}^{(v)}$, and $V_l^{(v)}$ is spanned by the basis functions $\psi_{h_l}^{(\mu)}$ which belong to the edges inside $\Omega_l^{(v)}$.

Then, successively for $v = 1, \ldots, M'_{h_l}$, we solve the least-squares problems

$$\min_{\delta p_l^{(v)} \in Q_l^{(v)}} \left\| \mathcal{R}(p_{h_l}^{(k)}, u_{h_l}^{(k)}) + \mathcal{J}(p_{h_l}^{(k)}, u_{h_l}^{(k)}) \begin{pmatrix} \tilde{\delta p}_{h_l} + \delta p_l^{(v)} \\ \tilde{\delta u}_{h_l} \end{pmatrix} \right\|_{0,\Omega}^2$$

and update $\tilde{\delta p}_{h_l}$ by $\tilde{\delta p}_{h_l} + \delta p_l^{(v)}$. After that we solve, again for $v = 1, \ldots, M'_{h_l}$,

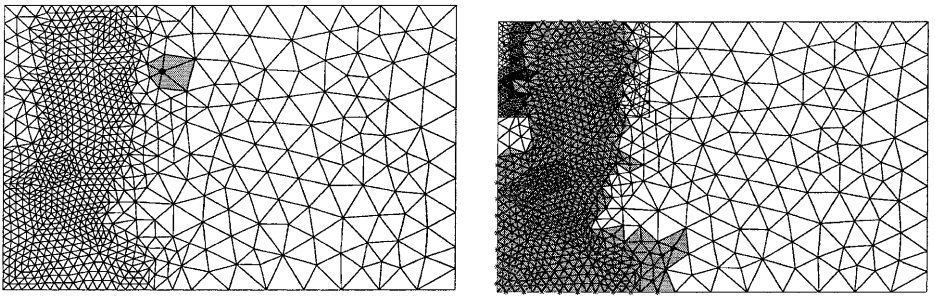

Figure 1. Local subdomain $\Omega_l^{(v)}$ and active points for the second refinement level

$$\min_{\delta u_l^{(v)} \in V_l^{(v)}} \left\| \mathscr{R}(p_{h_l}^{(k)}, u_{h_l}^{(k)}) + \mathscr{J}(p_{h_l}^{(k)}, u_{h_l}^{(k)}) \begin{pmatrix} \tilde{\delta} p_{h_l} \\ \tilde{\delta} u_{h_l} + \delta u_l^{(v)} \end{pmatrix} \right\|_{0,\Omega}^2$$

and update $\tilde{\delta} u_{h_l}$ by $\tilde{\delta} u_{h_l} + \delta u_l^{(v)}$. In other words, the linearized least-squares functional is successively minimized with respect to low-dimensional subspaces ($\dim Q_l^{(v)} = 1$ and $\dim V_l^{(v)}$ is typically between 5 and 8 for most of the points).

The second type of smoothing iteration differs from the above one in that it simultaneously minimizes with respect to both local subspaces. That is, for $v = 1, \ldots, M'_{h_l}$, we successively solve the least-squares problems

$$\min_{\delta p_l^{(v)} \in Q_l^{(v)}, \delta u_l^{(v)} \in V_l^{(v)}} \left\| \mathscr{R}(p_{h_l}^{(k)}, u_{h_l}^{(k)}) + \mathscr{J}(p_{h_l}^{(k)}, u_{h_l}^{(k)}) \begin{pmatrix} \tilde{\delta} p_{h_l} + \delta p_l^{(v)} \\ \tilde{\delta} u_{h_l} + \delta u_l^{(v)} \end{pmatrix} \right\|_{0,\Omega}^2$$

and update $\tilde{\delta} p_{h_l}$ and $\tilde{\delta} u_{h_l}$ by $\tilde{\delta} p_{h_l} + \delta p_l^{(v)}$ and $\tilde{\delta} u_{h_l} + \delta u_l^{(v)}$, respectively. This amounts to the solution of a linear system of size $\dim Q_l^{(v)} + \dim V_l^{(v)}$ (typically between 6 and 9) for each point in the triangulation.

In order to avoid suboptimal complexity, those points $x_l^{(v)}$ on the fine level which satisfy

$$Q_l^{(v)} = Q_{l-1}^{(v)}, \quad V_l^{(v)} = V_{l-1}^{(v)}$$

should be skipped in the smoothing iteration. This means that only those points connected to at least one newly created fine level point are considered. This set of active points is shown in Fig. 1 for the second refinement level of the sequence of triangulations associated with the numerical example in the next section.

In order to illustrate the performance of the multilevel algorithms, we present the results of numerical tests for the linear least-squares problem

$$\min_{\hat{p}_h \in Q_h, \hat{u}_h \in V_h} \| \mathscr{R}(p^D + \hat{p}_h, u^N + \hat{u}_h) \|_{0,\Omega}^2$$

with

$$\mathscr{R}(p,u) = \begin{pmatrix} p - p^{\text{old}} + \tau \operatorname{div} u \\ \sqrt{\tau}(u + \nabla p) \end{pmatrix}.$$

Obviously, this is the first-order system least-squares formulation of a linear heat equation. Since we want to show the effectiveness of the method in an adaptive setting, we consider this linear least-squares problem on the sequence of triangulations resulting from the refinement strategy in the example studied in Section 5 (see Fig. 3). Tables 1 and 2 give the asymptotic convergence factors (spectral radius of the iteration operator) for an adaptive multilevel V-cycle algorithm with one pre-smoothing and one post-smoothing step. The Gauss–Seidel iteration described above is used in the pre-smoothing phase (using the ordering of the points according to the construction of the triangulation). In the post-smoothing phase, the same Gauss–Seidel iteration is performed with the reverse ordering of the points. This leads to a symmetric V-cycle iteration operator and the spectral radius is therefore an upper bound for the actual reduction of the algebraic error in each step. Of particular interest is the dependence of the convergence rate on the refinement level l and on the parameter τ.

The numbers in Tables 1 and 2 show the average error reduction factors of the V-cycle method after a number of iterations (usually about 12 to 15). Obviously, there is only a marginal difference between the performance of both smoothing methods inside the V-cycle algorithm.

For the computational experiments in the following section, we exploit the multilevel structure again by imbedding the Gauss–Newton method into a nested iteration, i.e., we use the approximation on the next coarser level as a starting guess. If

Table 1. Convergence rate of the adaptive multilevel method using smoothing algorithm 1

	$\tau = 10^{-2}$	$\tau = 1$	$\tau = 10^{2}$
$l = 1$	0.17	0.31	0.31
$l = 2$	0.27	0.32	0.32
$l = 3$	0.28	0.28	0.28
$l = 4$	0.32	0.33	0.33
$l = 5$	0.35	0.35	0.35

Table 2. Convergence rate of the adaptive multilevel method using smoothing algorithm 2

	$\tau = 10^{-2}$	$\tau = 1$	$\tau = 10^{2}$
$l = 1$	0.17	0.31	0.31
$l = 2$	0.27	0.32	0.31
$l = 3$	0.27	0.28	0.28
$l = 4$	0.32	0.33	0.33
$l = 5$	0.35	0.35	0.35

$$[p_l, u_l] = \texttt{gaussn}(l, p_l^{\text{start}}, u_l^{\text{start}})$$

denotes the Gauss–Newton method on level l starting with $(p_l^{\text{start}}, u_l^{\text{start}})$ and providing the approximate solution (p_l, u_l), then this algorithm has the form

$$\begin{aligned}
&(p_{-1}, u_{-1}) = (p_0^{\text{old}}, u_0^{\text{old}});\\
&\texttt{for } l = 0 : L,\\
&\quad (p_l^{\text{start}}, u_l^{\text{start}}) = (p_{l-1}, u_{l-1});\\
&\quad [p_l, u_l] = \texttt{gaussn}(l, p_l^{\text{start}}, u_l^{\text{start}});\\
&\quad \texttt{end}
\end{aligned}$$

5. Computational Experiments

In this section, we present numerical results with the adaptive multilevel V-cycle algorithm for our nonlinear least-squares problem using the two types of Gauss–Seidel smoothers described in the previous section. For these tests, we use a water table recharge problem as described in [16] which models infiltration into initially dry sand. The computational domain is a box of 3 m length and 2 m depth as sketched in Fig. 2.

At time $t = 0$ we assume a constant hydraulic potential at -1.7 m (which is the position of the groundwater table). For $t > 0$ we have constant infiltration of 0.148 m/h through the boundary segment Γ_1. Zero flux boundary conditions are prescribed at the boundary segments Γ_2, Γ_3 and Γ_4, while the hydraulic potential is held constant at -1.7 m at the right boundary Γ_5.

We use the model by van Genuchten [15] with the parameters listed in [6] for the functions $K(p)$ and $\theta(p)$. For some types of soil (e.g. sand), this parametrization

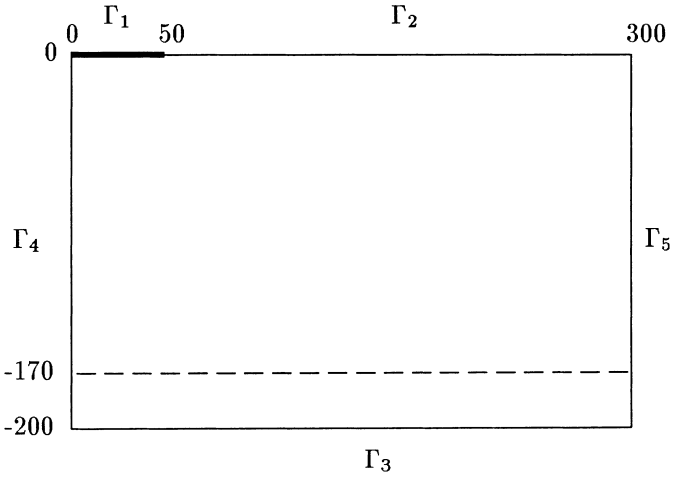

Figure 2. Test example of a two-dimensional water table recharge problem

leads to unbounded $K'(p)$ in the saturated limit which causes problems for the Newton iteration. Following a suggestion in [8, Chap. 6], we replace $K(p)$ by a cubic spline interpolant in a neighborhood of the saturated limit (for $0 \leq z - p \leq 10^{-2}$ where z is the height). We also found it useful to limit the permeability from below by $10^{-3}K_s$.

Our interest is in the performance of the multilevel solvers for the linearized least-squares problems inside the Gauss–Newton iteration. For fixed $\tau = 0.1$, we pick the step from 3.9 hours to 4 hours from the simulation and concentrate on the solution of the corresponding nonlinear elliptic problem (2) at this time step. We use the adaptive refinement strategy described in Section 2 with $\varepsilon = 5 \cdot 10^{-8}$ and $L = 5$. The final triangulation after five levels of refinement is shown in Fig. 3.

Table 3 shows the number of degrees of freedom (for u_h and for p_h) and the minimum of the least-squares functional on the different levels.

Table 4 shows the number of Gauss–Newton steps and the total number of V-cycles on each level required to satisfy the stopping criterion (8) with $\eta = 10^{-2}$ for both versions of the adaptive multilevel method. Note that these are the numbers inside the nested iteration algorithm presented at the end of the previous section, i.e., we already start from a good initial guess, in general.

The results in Table 4 show that the number of Gauss–Newton steps remains rather small but increases on the finest level. However, the total number of

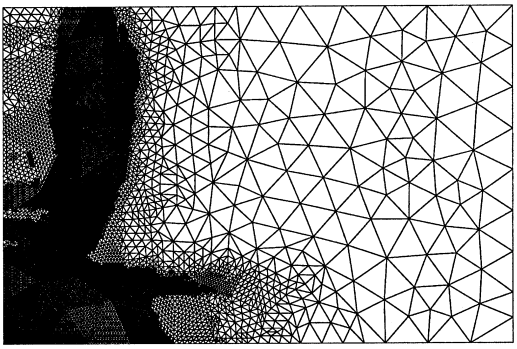

Figure 3. Triangulation after 5 levels of adaptive refinement

Table 3. Degrees of freedom and least-squares functional on different levels after 4 hours

	dim V_h	dim Q_h	$\|\mathscr{R}(p^D + \hat{p}_h, u^N + \hat{u}_h)\|^2_{0,\Omega}$
$l = 0$	485	177	$5.69 \cdot 10^{-5}$
$l = 1$	1102	396	$2.69 \cdot 10^{-5}$
$l = 2$	3217	1125	$1.04 \cdot 10^{-5}$
$l = 3$	10171	3481	$4.00 \cdot 10^{-6}$
$l = 4$	29364	9928	$1.33 \cdot 10^{-6}$
$l = 5$	84052	28226	$4.21 \cdot 10^{-7}$

Table 4. Number of Gauss–Newton steps and total number of V-cycles in the multilevel method

	Algorithm 1		Algorithm 2	
	Gauss–Newton steps	V-cycles	Gauss–Newton steps	V-cycles
$l = 0$	13	13	13	13
$l = 1$	11	22	11	23
$l = 2$	8	16	7	14
$l = 3$	4	12	6	17
$l = 4$	4	21	4	18
$l = 5$	13	52	13	41

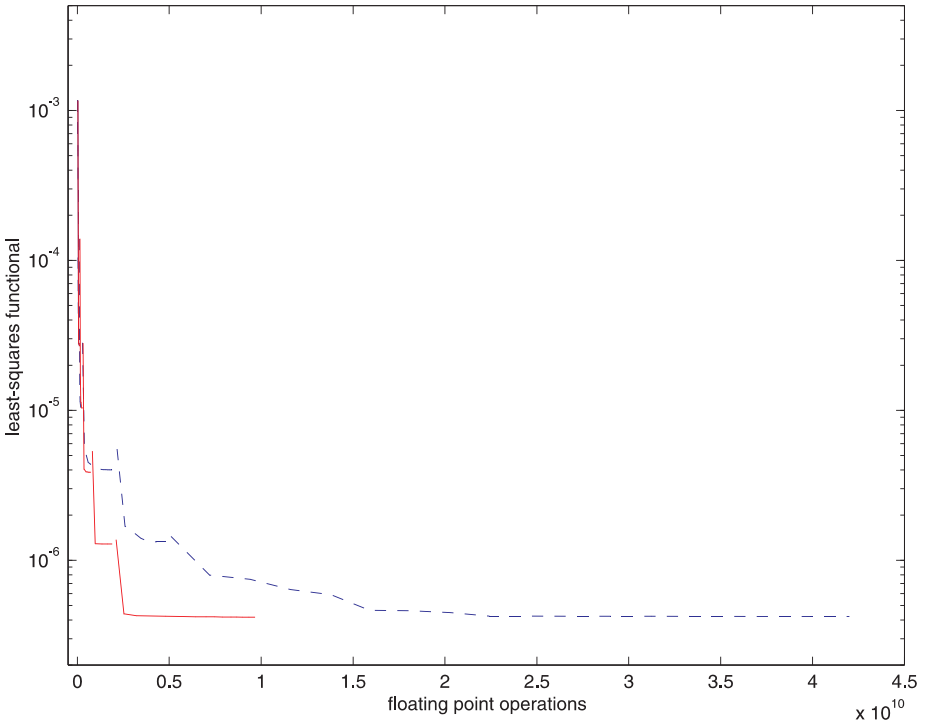

Figure 4. Least-squares functional vs. computational work

V-cycles is growing at a higher rate than the number of Gauss–Newton iterations as the mesh is refined. This is in contrast to the results in Tables 1 and 2 of the previous section which suggest the convergence to be level-independent. We suspect that this slower convergence of the multilevel V-cycle on finer levels in our example is caused by the large variations in the coefficients (mainly $K(p_h)$).

Figure 4 shows a comparison of both types of multilevel algorithms (solid line) compared to an exact Gauss–Newton method using a sparse direct solver (dashed line). The multilevel method using the second type of smoothing algorithm was marginally faster but the convergence curves in 4 are completely indistinguishable.

In both cases, the size of the nonlinear least-squares functional (our overall error measure) is plotted against computational work measured in floating number operations. In each case, the five curves show the functional reduction on levels $l = 1$ to 5. Some of the additional work (Gauss–Newton method on level 0, construction of refined triangulation etc.), not shown since it is identical for both methods, is responsible for the gaps in the graphs.

The jump from one level to the next seen in Fig. 4 comes from the fact that in our implementation we actually minimize an approximation $\|\mathscr{R}_h(\cdot,\cdot)\|^2_{0,\Omega}$ instead of $\|\mathscr{R}(\cdot,\cdot)\|^2_{0,\Omega}$ on the triangulation $\mathscr{T}_h$. This approximate least-squares functional results from replacing $K(p_h)$ and $\theta(p_h)$ by piecewise linear interpolants $K_h(p_h)$ and $\theta_h(p_h)$, respectively. One of the consequences of the use of this approximate least-squares functional is that, in general,

$$\|\mathscr{R}_{h_{l+1}}(p^D + \hat{p}_{h_l}, u^N + \hat{u}_{h_l})\|^2_{0,\Omega} > \|\mathscr{R}_{h_l}(p^D + \hat{p}_{h_l}, u^N + \hat{u}_{h_l})\|^2_{0,\Omega},$$

particularly on coarse levels. Figure 4 shows that in our numerical example there is almost no increase of the functional anymore when moving from level $l = 4$ to $l = 5$. This suggests that piecewise linear interpolation produces a sufficiently good approximation of the functional at this fine resolution.

Acknowledgement

I thank Johannes Korsawe and an anonymous referee for helpful suggestions.

References

[1] Arnold, D. N., Falk, R. S., Winther, R.: Preconditioning in H(div) with applications. Math. Comp. *66*, 957–984 (1997).
[2] Berndt, M., Manteuffel, T. A., McCormick, S. F.: Local error estimates and adaptive refinement for first-order system least squares. Electr. Trans. Numer. Anal. *6*, 35–43 (1997).
[3] Braess, D.: Finite elements. Cambridge: Cambridge University Press 1997.
[4] Brezzi, F., Fortin, M.: Mixed and hybrid finite element methods. New York: Springer 1991.
[5] Cai, Z., Lazarov, R., Manteuffel, T. A., McCormick S. F.: First-order system least squares for second-order partial differential equations: Part I. SIAM J. Numer. Anal. *31*, 1785–1799 (1994).
[6] Carsel R. F., Parrish, R. S.: Developing joint probability distributions of soil water retention characteristics. Water Resources Res. *24*, 755–769 (1988).
[7] Dennis, J. E., Schnabel, R. B.: Numerical methods for unconstrained optimization and nonlinear equations. Philadelphia: SIAM 1996.
[8] Fuhrmann, J.: Zur Verwendung von Mehrgitterverfahren bei der numerischen Behandlung elliptischer partieller Differentialgleichungen mit variablen Koeffizienten, PhD thesis, Technische Universität Chemnitz-Zwickau, Aachen 1995.
[9] Helmig, R.: Multiphase flow and transport processes in the subsurface. Berlin Heidelberg New York Tokyo: Springer 1997.
[10] Korsawe, J., Starke, G.: Multilevel projection methods for nonlinear least-squares finite element computations. Electr. Trans. Numer. Anal. (1999) (to appear).
[11] Mualem, Y.: A new model for predicting the hydraulic conductivity of unsaturated porous media. Water Resources Res. *12*, 513–522 (1976).
[12] Raviart, P. A., Thomas, J. M.: A mixed finite element method for second order elliptic problems. In: Mathematical aspects of the finite element method (Galligani, E. M. I., ed.), pp. 292–315. Berlin Heidelberg New York: Springer, 1977.
[13] Starke, G.: Adaptive least-squares Galerkin methods for parabolic problems. SIAM J. Numer. Anal. (in preparation).

[14] Starke, G.: Least-squares mixed finite element solution of variably saturated subsurface flow problems. SIAM J. Sci. Comput. *20* (to appear).
[15] Van Genuchten, M. T.: A closed-form equation for predicting the hydraulic conductivity of unsaturated soils. Soil Sci. Soc. Am. J. *44*, 892–898 (1980).
[16] Vauclin, M., Khanji, D., Vachaud, G.: Experimental and numerical study of a transient, two-dimensional unsaturated-saturated water table recharge problem. Water Resources Res. *15*, 1089–1101 (1979).

Gerhard Starke
Fachbereich Mathematik
Universität-GH Essen
45117 Essen
Germany
e-mail: starke@ing-math.uni-essen.de